*Exploration Geophysics (2006) **37**, 30-36*
Butsuri-Tansa (Vol. 59, No. 1)
Mulli-Tamsa (Vol. 9, No. 1)

Time-lapse crosswell seismic tomography for monitoring injected CO_2 in an onshore aquifer, Nagaoka, Japan

Hideki Saito [1] **Dai Nobuoka** [1] **Hiroyuki Azuma** [1] **Ziqiu Xue** [2] **Daiji Tanase** [3]

Key Words: time-lapse, crosswell, seismic tomography, CO_2 injection, onshore aquifer, Nagaoka

ABSTRACT

Japan's first pilot-scale CO_2 sequestration experiment has been conducted in Nagaoka, where 10 400 t of CO_2 have been injected in an onshore aquifer at a depth of about 1100 m. Among various measurements conducted at the site for monitoring the injected CO_2, we conducted time-lapse crosswell seismic tomography between two observation wells to determine the distribution of CO_2 in the aquifer by the change of P-wave velocities. This paper reports the results of the crosswell seismic tomography conducted at the site.

The crosswell seismic tomography measurements were carried out three times; once before the injection as a baseline survey, and twice during the injection as monitoring surveys. The velocity tomograms resulting from the monitoring surveys were compared to the baseline survey tomogram, and velocity difference tomograms were generated. The velocity difference tomograms showed that velocity had decreased in a part of the aquifer around the injection well, where the injected CO_2 was supposed to be distributed. We also found that the area in which velocity had decreased was expanding in the formation up-dip direction, as increasing amounts of CO_2 were injected. The maximum velocity reductions observed were 3.0% after 3200 t of CO_2 had been injected, and 3.5% after injection of 6200 t of CO_2.

Although seismic tomography could map the area of velocity decrease due to CO_2 injection, we observed some contradictions with the results of time-lapse sonic logging, and with the geological condition of the cap rock. To investigate these contradictions, we conducted numerical experiments simulating the test site. As a result, we found that part of the velocity distribution displayed in the tomograms was affected by artefacts or ghosts caused by the source-receiver geometry for the crosswell tomography in this particular site. The maximum velocity decrease obtained by tomography (3.5%) was much smaller than that observed by sonic logging (more than 20%). The numerical experiment results showed that only 5.5% velocity reduction might be observed, although the model was given a 20% velocity reduction zone. Judging from this result, the actual velocity reduction can be more than 3.5%, the value we obtained from the field data reconstruction. Further studies are needed to obtain more accurate velocity values that are comparable to those obtained by sonic logging.

[1] *Oyo Corporation*
43 Miyukigaoka, Tsukuba, Ibaraki 305-0841, Japan
Phone: +81-29-851-6621
Facsimile: +81-29-851-5450
Email: saito-hideki@oyonet.oyo.co.jp

[2] *Research Institute of Innovative Technology for the Earth (RITE)*
9-2 Kizugawadai, Kizu-cho, Soraku-gun, Kyoto 619-0292, Japan

[3] *Engineering Advancement Association of Japan (ENAA)*
1-4-6 Nishi-Shinbashi, Minato-ku, Tokyo 105-0003, Japan

Manuscript received January 9, 2006; accepted January 30, 2006. Part of this paper was presented at the 112th SEGJ Conference (2005).

INTRODUCTION

Japan's first pilot-scale CO_2 sequestration experiment has been conducted in Nagaoka, where 10 400 t of CO_2 have been injected in an onshore aquifer at a depth of about 1100 m. An outline of the project and the geology of the site are given by another paper in this issue (Xue et al., 2006). It is very important for the geological sequestration project to monitor the distribution of the injected CO_2 in the aquifer. Although this paper reports Japan's first experience with CO_2 sequestration experiments, there have been other reported examples of seismic monitoring of CO_2 injection projects. For example, Eiken (2004) showed that time-lapse 3D seismic reflection surveys had been successfully applied in the Sleipner project, where 5 Mt of CO_2 had been injected in an offshore aquifer at a depth of about 1000 m. The distribution of injected CO_2 was revealed by seismic reflection amplitude and P-wave velocity changes. Another example was reported by White (2004), who described time-lapse 3D seismic surveys that had been successfully applied in the Weyburn project. P-wave velocity and reflection amplitude changes had been observed, associated with the injection of 5 Mt of CO_2 into an onshore oil reservoir at a depth of about 1500 m. Although these results showed the applicability of P-wave velocity changes to the monitoring of injected CO_2 distribution, the amount of CO_2 planned to be injected at our Nagaoka site was so small (in total, 10 400 t of CO_2), especially at the early stages, that we needed much higher resolution compared to surface seismic surveys. That is one of the reasons why we decided to apply crosswell seismic tomography to monitor the injected CO_2 distribution. The usefulness of seismic velocity measurements for the detection of injected CO_2 was also supported by core velocity measurements (e.g., Xue and Ohsumi, 2004). Xue and Ohsumi reported that a reduction of more than 10% in P-wave velocities is expected from CO_2 injection, and suggested that the movement of injected CO_2 in the aquifer may be detectable by crosswell seismic measurements. They also concluded that the velocity change caused by CO_2 saturation might be distinguished from the velocity change resulting from pore pressure build-up from CO_2 injection, because the latter is much smaller than the former. Because well logging is one of the reliable methods of detecting CO_2 breakthrough at an observation well, time-lapse well logging was conducted during CO_2 injection in this project (Xue et al., 2006). We can use the sonic logging data to verify or calibrate our tomography results. Although crosswell seismic tomography has been successfully applied to monitor injected CO_2 in enhanced oil recovery operations (Harris et al., 1995; Hoversten et al., 2003), there are few examples of the application of crosswell seismic tomography for the purpose of CO_2 sequestration monitoring at an onshore aquifer site. In this paper, the results of time-lapse crosswell seismic tomography are demonstrated and discussed with numerical experiments.

TIME-LAPSE CROSSWELL SEISMIC TOMOGRAPHY

The baseline survey (BLS) for crosswell seismic tomography was conducted in February 2003, before CO_2 injection started in July 2003. The first monitoring survey (MS1) was conducted in January 2004, after 3200 t of CO_2 had been injected, and the second monitoring survey (MS2) was conducted in July 2004, after 6200 t of CO_2 had been injected.

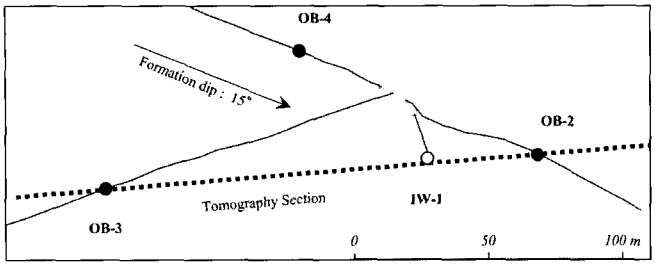

Fig. 1. Well trajectories of the injection well (IW-1) and observation wells (OB-2, OB-3, and OB-4) at the Nagaoka test site. The rectangles show the well positions at the ground surface, and the circles show the well position at the depth of the target aquifer (about 1100 m below the ground surface) for each well. Crosswell seismic tomography was conducted in a vertical section between the wells OB-2 and OB-3 as shown by a broken line.

Source and Receiver Geometry

Figure 1 shows the trajectories of the observation wells used in the tomography measurements and the seismic tomography section. Figure 2 shows the source and receiver configurations in horizontal, front, and side views. Although the two observation wells are not vertical and parallel, the deviation from the vertical is so small that two-dimensional tomography is considered to be applicable. Crosswell distance at the depth of the target aquifer is about 160 m. Source positions were set every 4 m between 900 and 1284 m depth in OB-2. Receiver positions were set every 4 m between 900 and 1228 m depth in OB-3. The CO_2 injection point at a depth of about 1100 m is also shown in Figure 2.

Data Acquisition

The energy source used was an Oyo Wappa Source (Yokota et al., 2000), a multidisk-type downhole mechanical source which can provide good repeatability, and generated high frequencies (up to 500 Hz) with sufficient energy at this site. A 24-sensor hydrophone array cable was used as a receiver. Oyo's DAS-1 was used for data acquisition, with 0.125 msec sampling. Since the energy of first arrival waves is very small, stacking (averaging) of up to 20 signals was done to improve signal-to-noise ratio. Data acquisition for the crosswell measurements took about one week of 24-hour operation every day.

Data Analysis

Before the tomographic reconstruction, the first arrival traveltimes were picked up from the waveform data. Traveltime picking was done manually and the traveltime curves were carefully checked and adjusted. Figure 3 shows all the traveltime curves for first arrivals picked for the baseline survey. The first arrival traveltime curves obtained by crosswell measurements in 2D velocity structures must have some characteristics which arise from a fundamental rule that traveltime data acquired with similar observation geometry should be almost uniform (Saito, 1992). Almost all traveltime curves in Figure 3 satisfy such requirements.

Since the sources and receivers were not exactly on a vertical plane because of well deviations, those positions were projected onto a vertical plane containing the tops of the aquifer at the two observation wells, as shown in Figure 2. Before the tomographic inversion, the vertical section was divided into small rectangular cells, 4 m in height by 8 m width, to express the velocity distribution by assigning a constant velocity in each cell. The cell width was determined by our experience that a proper velocity distribution can be reconstructed when the width of each cell is larger than 1/20 of the crosswell distance (Saito, 2001).

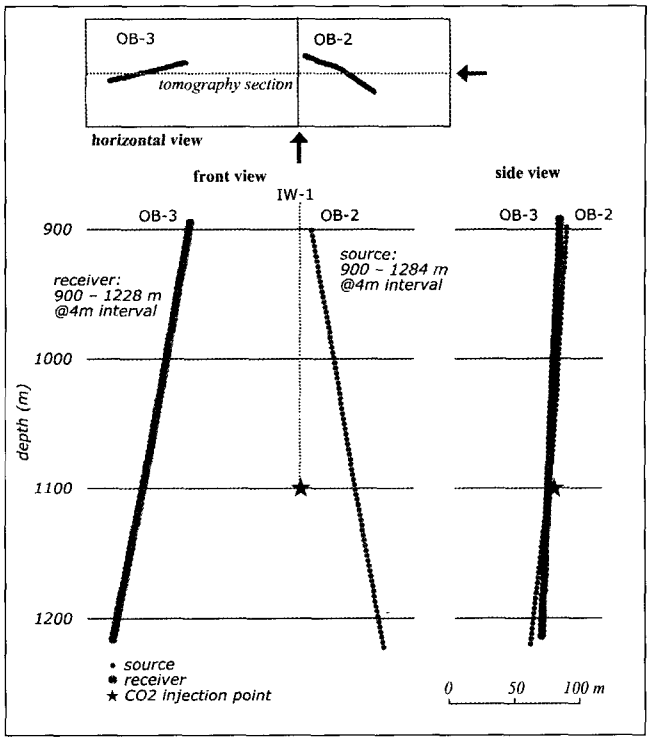

Fig. 2. The source and receiver configurations in horizontal, front, and side views.

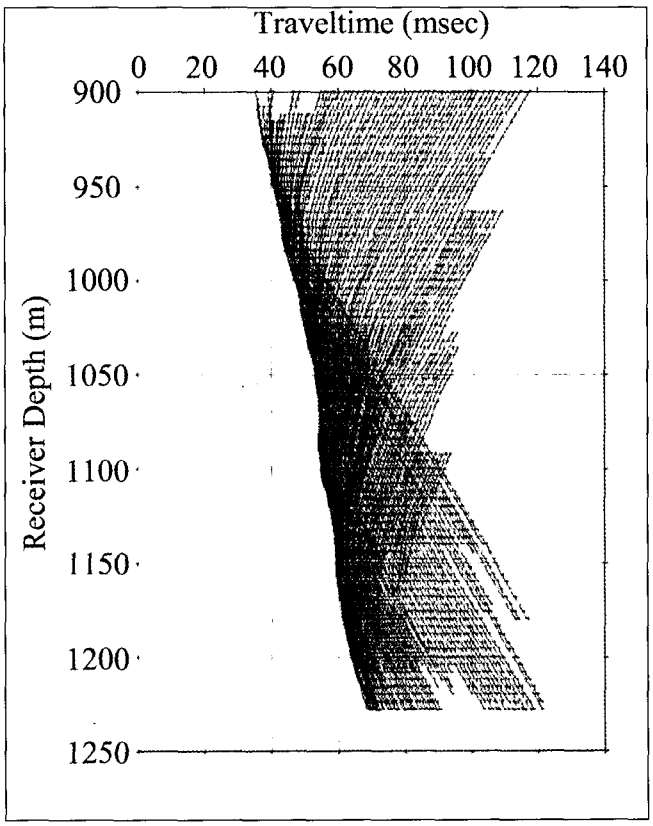

Fig. 3. Traveltime curves for first arrivals picked from the baseline survey.

Tomographic inversion was done using an iteratively linearising algorithm, in which refracted ray paths were taken into account. First arrival traveltimes and ray path calculations in this study used methods developed by Saito (1989) and referred to as the "Huygens' method" (Saito, 2001). The method is called "ray tracking" rather than "ray tracing", because the first step of the computation procedure calculates the wavefront emanating from

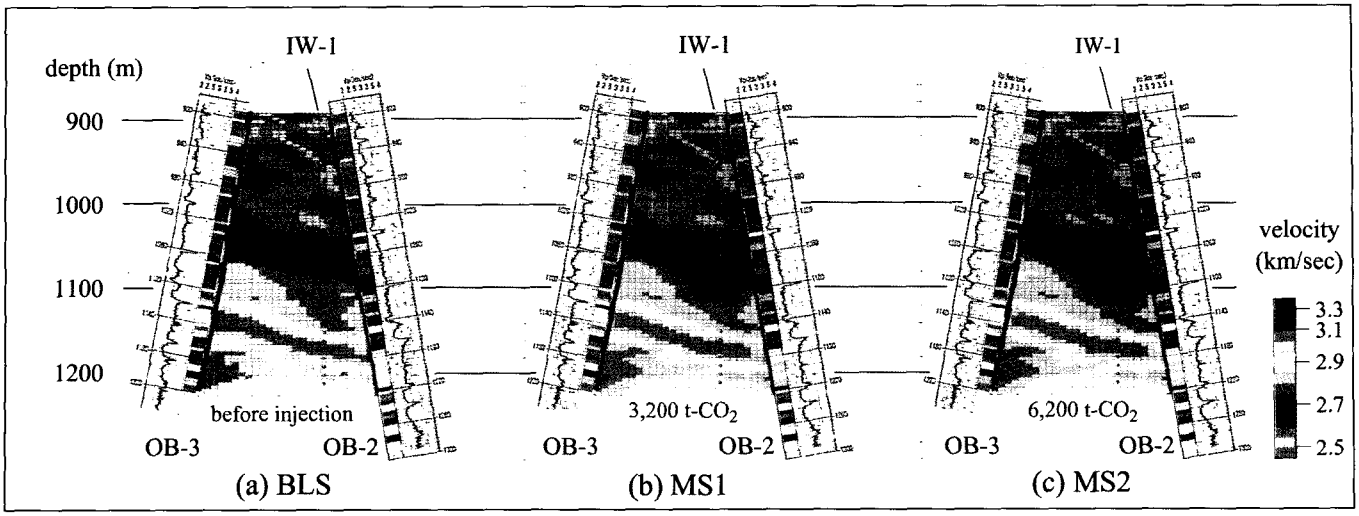

Fig. 4. Velocity tomograms for BLS (a), MS1 (b), and MS2 (c). Coloured columns along the wells OB-2 and OB-3 show the sonic log velocities obtained before CO_2 injection. The same colour scale is used in the velocity tomograms and the sonic logs.

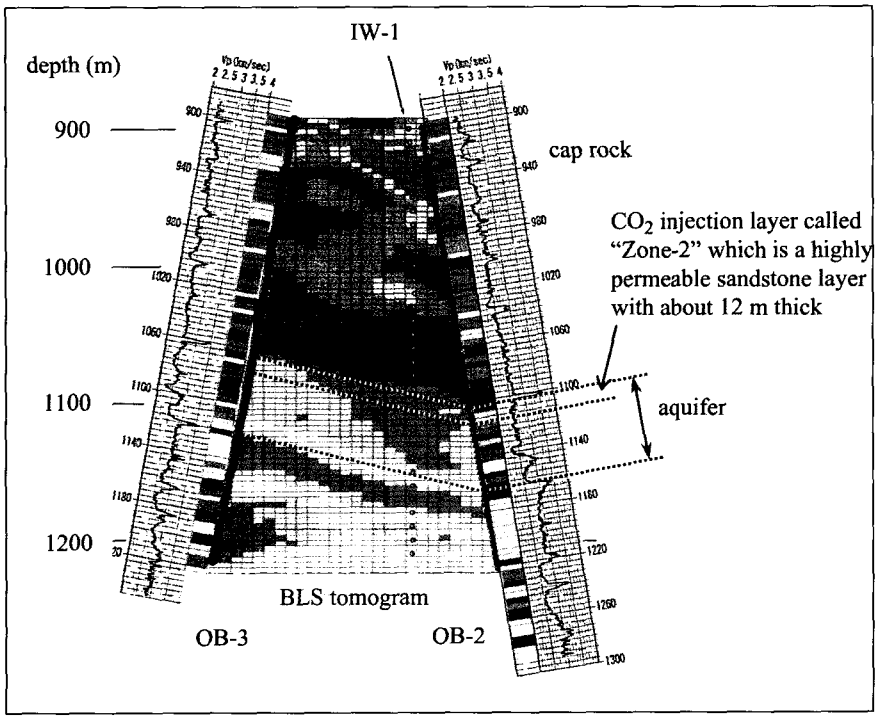

Fig. 5. The locations of the aquifer and CO_2 injection target layer projected onto the BLS tomogram.

the source point throughout the velocity model, and then backtracks from each receiving point along the ray path to the source. One of the features of this method is the applicability to any velocity structures, including those with high velocity contrasts, and to any source-receiver geometries. Another advantage is the capability to calculate traveltimes and ray paths of head waves where they are first arrivals. The method only considers geometric rays which assume that the propagating waves have a high-frequency limit. Any wave volumes such as so-called Fresnel zones (e.g., Spetzler and Sneider, 2004) are not taken into account in this study.

The first step of the tomographic inversion is to create an initial velocity model. For this purpose, the Back Projection Technique (BPT) was used. Beginning from the initial velocity model, the iterative tomographic reconstruction with ray tracing updated the velocity model after each iteration. The Modified Simultaneous Iterative Reconstruction Technique (Modified-SIRT), which is very capable of imaging high velocity contrasts (Sanny and Sassa, 1992), was used as a velocity update algorithm. The BPT model was used as an initial velocity model for the baseline survey analysis, and the baseline survey tomogram was used as an initial model for the monitoring surveys. Twenty iterations were performed for the baseline survey reconstruction, and 10 iterations were performed for each monitoring survey.

Time-lapse tomography results

Figure 4 shows the velocity tomograms for BLS, MS1, and MS2. Coloured columns along the wells OB-2 and OB-3 show the sonic log velocity obtained before CO_2 injection, using the same colour scale as the velocity tomograms. Figure 5 shows the locations of the aquifer and the CO_2 injection target layer projected onto the BLS tomogram. The sonic logs show a thin (less than 4 m) high-velocity layer at the top of the aquifer. However, this layer was not reconstructed by seismic tomography, because it is too thin to be detected by a crosswell survey with this observation geometry. In fact, we could not observe head waves from the high-velocity layer in the waveform data for any source-receiver pairs. The tomography velocity and sonic log velocity correlated well with each other, except at thin layers.

In order to clarify the velocity changes between those monitoring stages, velocity difference tomograms were created as shown in Figure 6. The velocity changes between baseline and monitoring surveys were defined in each cell by:

$$\text{velocity difference}(\%) = \frac{\left(V_{MS} - V_{BLS}\right)}{V_{BLS}} \times 100 \ , \qquad (1)$$

where V_{BLS} is the velocity in the baseline survey tomogram and V_{MS} is the velocity in each monitoring survey tomogram.

In the vicinity of the injection well IW-1, each difference tomogram shows an area in the aquifer in which velocity has decreased. The maximum velocity reductions observed in the difference tomograms were 3.0% for the MS1 and 3.5% for the MS2. As the amount of injected CO_2 increased, the area of velocity reduction expanded, especially in the formation up-dip direction.

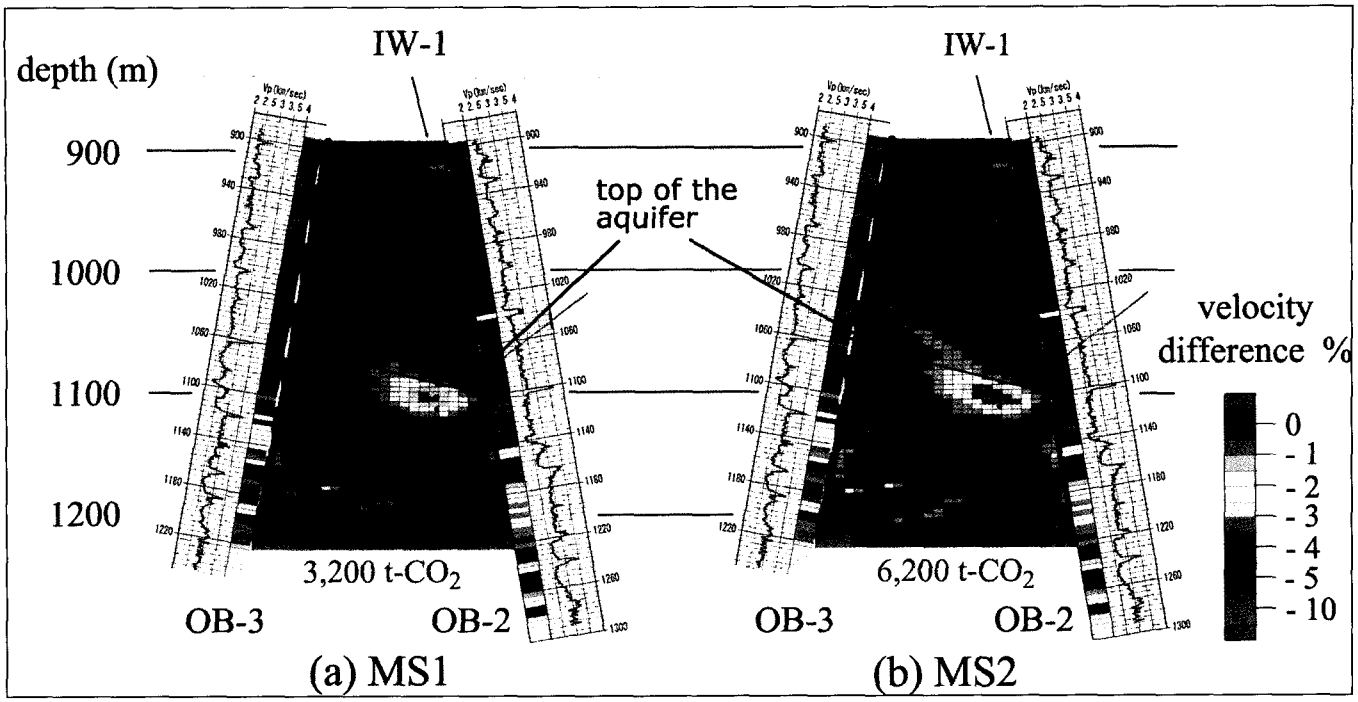

Fig. 6. Velocity difference tomograms: (a) Velocity difference between baseline and MS1 (after injection of 3200 t of CO_2) surveys. (b) Velocity difference between baseline and MS2 (after injection of 6200 t of CO_2) surveys.

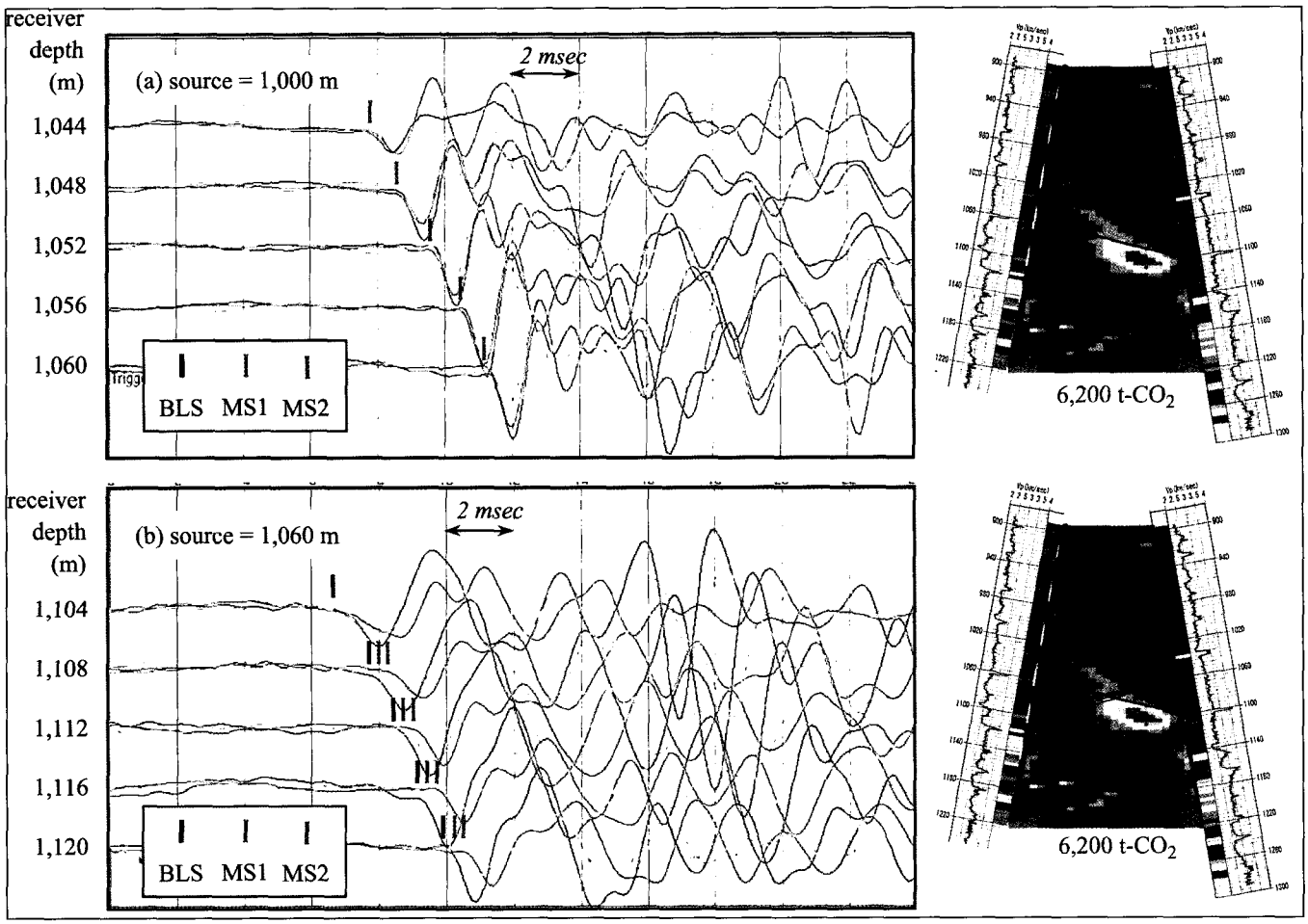

Fig. 7. Common-shot gather waveform data. (a) Source position is 1000 m and receivers are every 4 m between 1044 and 1060 m. (b) Source position is 1060 m and receivers are every 4 m between 1104 and 1120 m. At each depth the three traces shown in black, red, and blue correspond to the waveforms obtained at the BLS, MS1, and MS2 stages, respectively. The figure on the right shows ray paths for these five source-receiver pairs calculated using the MS2 velocity distribution and overlaid on the MS2 tomogram.

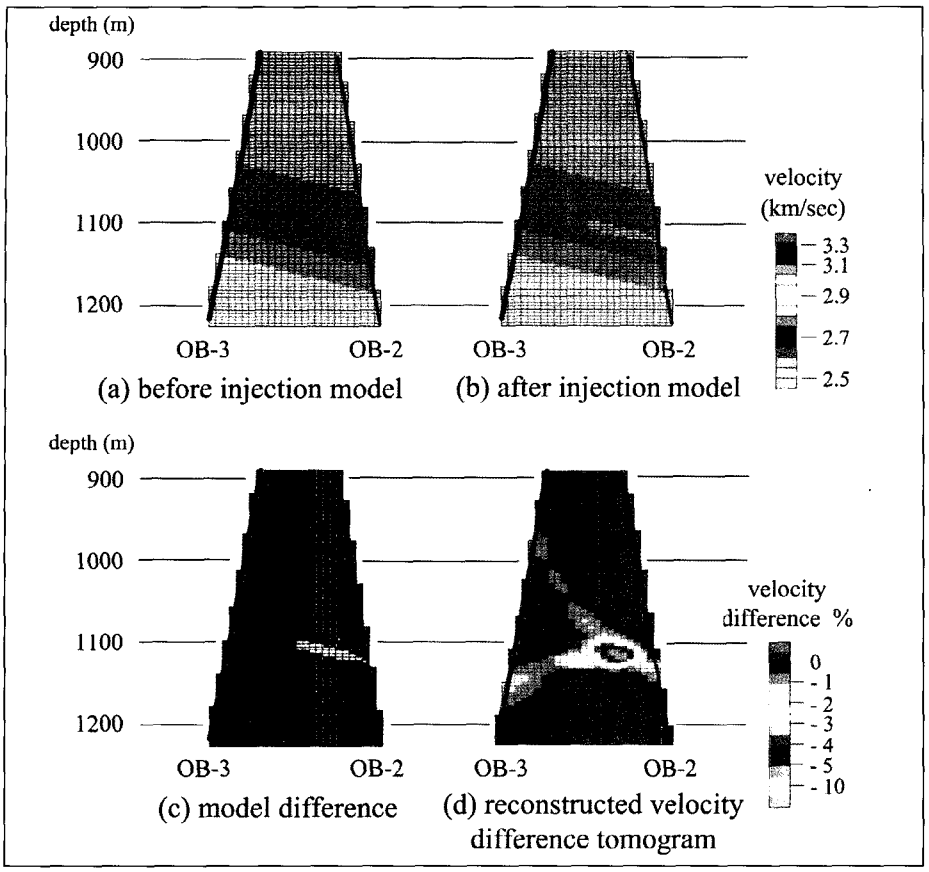

Fig. 8. Numerical experiment results. Source-receiver configurations used in the numerical experiments were the same as those used in the actual field geometry. (a) Baseline model. (b) Monitoring model. Velocity reduction from the baseline was set to be -20%. Maximum thickness of the low-velocity zone was 12 m. The thickness around OB-2 was set to be 4 m. (c) Velocity difference between two models. (d) Velocity difference tomogram.

From these observations, we interpreted the area of reduced velocity as the distribution of injected CO_2 within the aquifer.

To verify that the area of velocity reduction reconstructed by tomography is really the result of the traveltime delay along ray paths passing through a low-velocity anomaly, seismic waveforms for identical source-receiver pairs, acquired at different monitoring stages, were directly compared. Figure 7 shows two examples of common-shot gather waveform data acquired at the stages BLS, MS1, and MS2. Figure 7(a) shows the waveform data whose common shot position is 1000 m. Receivers are located at every 4 m between 1052 and 1068 m deep. This is an example where the ray paths do not pass through the area of velocity change caused by CO_2 injection. The three traces at each depth, shown in black, red and blue, correspond to the waveforms obtained at the BLS, MS1, and MS2 stages, respectively. In this case, the first arrival waveforms are almost identical. We can say that these time-lapse measurement data do not show any traveltime delay. The figure on the right shows ray paths for these five source-receiver pairs, calculated using the MS2 velocity distribution and overlaid on the MS2 tomogram. Since both source and receivers are located much shallower than the aquifer in this case, this result was as expected. On the other hand, the common-shot gather with source depth at 1060 m in Figure 7(b), some data for rays that pass through the area of velocity reduction in the aquifer show the traveltime delay clearly. The area of velocity reduction has expanded to the region which those rays passed through.

DISCUSSION

Although it was shown that the time-lapse seismic tomography outlined an area in which velocity decreased because of CO_2 injection, the velocity reduction values did not agree with those obtained by sonic logging, and the shape of the area in which velocity had decreased area was unexpected. The following contradictions were observed in the difference tomograms:

1) Although CO_2 breakthrough had been observed at the OB-2 well by logging conducted before the MS2 tomography survey, the area of velocity reduction, reconstructed by tomography, did not reach the well.

(2) Although sonic logging results showed more than 20% velocity reduction after breakthrough, the velocity difference tomogram of MS2, conducted after the breakthrough, showed at most only 3.5% reduction.

(3) Although the CO_2 was injected into a thin permeable sandstone layer (see Figure 5), a part of the area of velocity decrease seems to extend into the cap rock and the lower layers.

In order to investigate these problems, we carried out numerical experiments. Figure 8(a) shows a velocity model for the baseline survey. Figure 8(b) shows a velocity model for the monitoring survey in which has a velocity is reduced by 20% over an area whose thickness is 12 m for most of the model, but thinner (4 m) just around the well on the right. The velocity differences between these two models are shown in Figure 8(c). First arrival traveltimes were calculated for the same source-receiver pairs as in the actual field measurements. By using the data sets as inputs, the same tomography program used for the field data analysis was conducted to reconstruct the velocity distributions. The resulting velocity tomograms were used to create a velocity difference tomogram, shown in Figure 8(d). Figure 8(d) shows a thicker low-velocity zone than in the starting model (Figure 8(c)). The maximum velocity reduction obtained by tomographic inversion was 5.5%, although 20% had been set in the model. In addition, the area of reduced velocities does not reach the well on the right, perhaps because it is too thin to be detected by tomography. The results of the numerical experiment are summarised as follows:

(1) The numerical experiments demonstrated that seismic traveltime tomography could not detect an area in which velocity had decreased that was only 4 m thick, even if that area contacted the observation well. Because the time-lapse sonic logging showed velocity reduction only over a 5 m depth interval (Xue et al., 2006), it was difficult to detect such a thin zone by crosswell tomography, because of the limited resolution for this source-receiver geometry.

(2) The numerical experiments showed the maximum velocity reduction is about 5.5% though the velocity model has a 20% reduction zone. Judging from the result, the actual velocity reduction at the MS2 stage of injection could be larger than the 3.5% observed in the MS2 difference tomogram.

(3) The numerical experiment result showed some artefacts or ghosts from the velocity anomaly, in the upper left

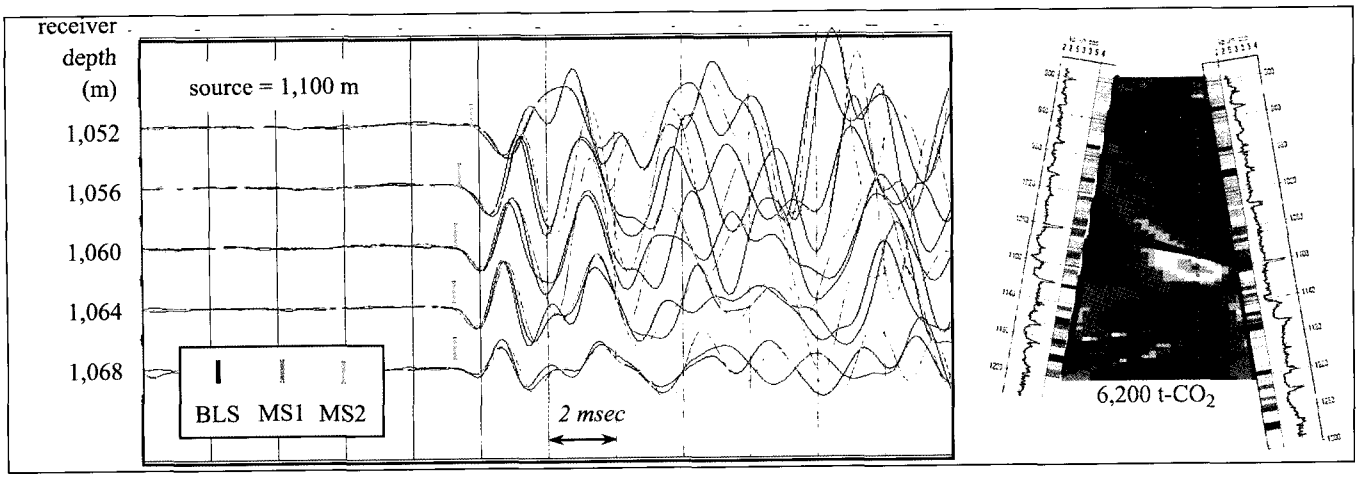

Fig. 9. Common-shot gather waveform data. Source position is 1100 m and receivers are every 4 m between 1052 and 1068 m. At each depth the three traces shown in black, red, and blue correspond to the waveforms obtained at the BLS, MS1, and MS2 stages, respectively. The figure on the right shows ray paths for these five source-receiver pairs calculated using the MS2 velocity distribution and overlaid on the MS2 tomogram.

and lower left directions. These have almost the same shapes as observed in the field results (Figure 6). As we did not add any noise to the numerical data, it is reasonable to suppose that these are artefacts caused by this geometry.

The other evidence that the extension of the area of velocity reduction in the upper left direction is an artefact is shown in Figure 9. This figure shows the waveform data whose common shot position is 1100 m, for receivers located every 4 m between 1052 and 1068 m. The figure on the right shows ray paths for these five source-receiver pairs, calculated using the MS2 velocity distribution and overlaid on the MS2 tomogram. In this case, the first arrival waveforms are almost identical. From this figure, we conclude that the apparent velocity anomaly extending in the upper left direction did not produce traveltime delays for rays passing through the area. This means that this apparent velocity anomaly must be an artefact.

CONCLUSIONS

Time-lapse crosswell seismic tomography was successfully applied to monitor injected CO_2 for the geological sequestration pilot project in Nagaoka, Japan. The velocity difference tomograms obtained before and after CO_2 injection revealed that the distribution of injected CO_2 in the aquifer can be imaged as area of velocity reduction. The velocity reductions resulting from CO_2 injection were found to be 3.0% for MS1 (after 3200 t of CO_2 injected) and 3.5% for MS2 (after 6200 t of CO_2 injected), by seismic tomography. However, these values disagreed with the results of time-lapse sonic logging, in which more than 20% velocity reduction had been observed after CO_2 breakthrough. The tomograms also showed a velocity anomaly extending into the cap rock, which is contrary to commonsense views of cap rock geology.

To investigate those contradictions, a numerical experiment was conducted. As a result, we found that the actual velocity reduction can be more than the 3.5% obtained from field data reconstruction, and that the apparent velocity anomaly extending into the cap rock is an artefact caused by this particular source-receiver geometry. The problem of velocity determination in a thin, low-velocity layer is one of the basic problems of traveltime tomography. However, some sophisticated inversion schemes, which include adequate constraints, can solve the problem (e.g., Lazaratos and Marion, 1997; Yokota et al. 2003).

After the MS2 survey reported in this paper, we have conducted three more crosswell seismic tomography surveys: MS3, after 8900 t of CO_2 had been injected; MS4, just after the end of the planned total 10400 t of CO_2 had been injected; and MS5, 10 months after the end of injection; but the results have not yet been compiled. From those results, we expect to obtain more valuable insights into the movement of the injected CO_2 in the aquifer.

ACKNOWLEDGMENTS

This work was supported by the Ministry of Economy, Trade and Industry of Japan under the contract for "Research and Development of Underground Storage for Carbon Dioxide". The authors thank all staff involved this project in ENAA, RITE, and Teikoku Oil Corporation. They also thank the anonymous reviewers and editors for their helpful comments and suggestions for improvement of the paper.

REFERENCES

Eiken, O., 2004, Review of geophysical monitoring results from the SACS project *presented at IEA Monitoring and Verification Workshop, Santa Cruz, November, 2004.*

Harris, J., Nolen-Hoeksema, R., Langan, R., Schaack, M., Lazaratos, S., and Rector III, J., 1995, High-resolution crosswell imaging of a west Texas carbonate reservoir: Part I – Project summary and interpretation: *Geophysics*, **60**, 667–681.

Hoversten, G., Gritto, R., Washbourne, J., and Daley, T., 2003, Pressure and fluid saturation prediction in a multicomponent reservoir using combined seismic and electromagnetic imaging: *Geophysics*, **68**, 1580–1591.

Lazaratos, S., and Marion, B., 1997, Crosswell seismic imaging of reservoir changes caused by CO_2 injection: *The Leading Edge*, **16**, 1300–1306.

Saito, H., 1989, Traveltimes and raypaths of first arrival seismic waves: Computation method based on Huygens' principle: *59th Annual International Meeting, Society of Exploration Geophysicists, Expanded Abstracts*, 244–247.

Saito, H., 1992, Characteristics of the first arrival traveltime curves obtained by crosshole seismic measurements: *Proceedings of the 86th SEGJ Conference*, 88–93.

Saito, H., 2001, *Seismic traveltime tomography for shallow subsurface explorations*: Ph.D. thesis (unpublished), Hokkaido University.

Sanny, T., and Sassa, K., 1994, Reduction of the effect of the near surface low velocity layer in tomographic imaging: *Proceedings of the 90th SEGJ Conference*, 84–88.

Spetzler, J., and Sneider, R., 2004, Tutorial: The Fresnel volume and transmitted waves: *Geophysics*, **69**, 653–663.

White, D., 2004, Seismic results from the Weyburn monitoring project: *presented at*

IEA Monitoring and Verification Workshop, Santa Cruz, November, 2004.

Xue, Z., and Ohsumi, T., 2004, Seismic wave monitoring of CO_2 migration in water-saturated porous sandstone: *Butsuri-Tansa (Geophysical Exploration)*, **57**, 25–32.

Xue, Z., Tanase, D., Watanabe, J., and Inoue, N., 2006, Time-lapse CO_2 monitoring well logging and quantitative evaluation of CO_2 saturation in an onshore aquifer, Nagaoka, Japan: *Exploration Geophysics*, **37**, (this issue).

Yokota, T., Ishii, Y., Shimada, S., Mizohata, S., Shoji, Y., Ohhashi, T., and Ogura, K., 2000, Development of a multi-disk type borehole seismic source – Aiming at practical applications for oil field survey - : *Butsuri-Tansa (Geophysical Exploration)*, **53**, 309–323.

Yokota, T., Nishida, A., Mizohata, S., Shimada, N., and Muraoka, S., 2003, Tomographic inversion for time-lapse oil reservoir monitoring: *Butsuri-Tansa (Geophysical exploration)*, **56**, 181–189.

長岡実証試験サイトの陸上帯水層に対するCO2圧入の繰り返し坑井間弾性波トモグラフィによるモニタリング

斎藤秀樹[1]・信岡　大[1]・東　宏幸[1]・薛　自求[2]・棚瀬大爾[3]

要　旨：　わが国初のCO2地中貯留実証実験が、長岡市で実施された。実験では、10,400tのCO2が深度約1,100mの陸域帯水層内に圧入された。実験サイトでは圧入されたCO2の挙動をモニタリングするために種々の計測が行われた。著者らはその一環として、２つの観測井を利用し、帯水層に圧入されたCO2の分布を弾性波（P波）速度の変化によってとらえるために、繰り返し坑井間弾性波トモグラフィを実施した。本稿は実験サイトで実施した坑井間弾性波トモグラフィの結果について報告するものである。

坑井間弾性波トモグラフィは、ベースライン探査として圧入前に1回、モニタリング探査として圧入中に2回、計3回実施した。モニタリング探査の速度トモグラムをベースライン探査の速度トモグラムと比較し、速度変化率トモグラムを作成した。速度変化率トモグラムには、圧入されたCO2が分布すると思われる帯水層内の圧入井周辺で、速度低下域が見られた。またCO2の圧入量の増加に伴って、速度低下域が地層の傾斜に沿って拡大していくことがわかった。弾性波トモグラフィによる速度低下率は、3,200tのCO2圧入後には3.0%、6,200t圧入後には3.5%であった。

弾性波トモグラフィによってCO2圧入による速度低下域をとらえられることがわかったが、同じサイトで実施された音波検層結果やこのサイトのキャップロックの地質状況などと対比すると、矛盾する点が見られた。そこで、それらの矛盾点を調べるため、数値実験を実施した。その結果、トモグラムに見られる速度低下域の一部は、本実験の起振点・受振点配置に起因する偽像であることがわかった。現場データのトモグラフィ解析で得られた速度低下率は最大で3.5%と、音波検層で得られた20%に比べて小さい値を示したが、本数値実験においては、モデルとして20%の速度低下を想定したにもかかわらず、トモグラフィ解析結果の最大速度低下率は5.5%であった。この結果から判断すると、実際の速度低下率は、トモグラフィ解析によって求められた3.5%より大きな値であることが推察される。音波検層速度との不一致については、今後もさらに検討を重ねる必要がある。

キーワード： time-lapse、坑井間、弾性波トモグラフィ、CO_2圧入、陸上帯水層

일본 Nagaoka의 육상 대수층에 주입된 CO_2의 관찰을 위한 시간차 시추공간 탄성파 토모그래피

Hideki Saito[1], Dai Nobuoka[1], Hiroyuki Azuma[1], Ziqiu Xue[2], and Daiji Tanase[3]

요　약：　일본의 첫 번째 파일럿 규모의 CO_2 격리실험이 Nagaoka 에서 약 1,100m 깊이의 육상 대수층에 10,400 톤의 CO_2 를 주입하면서 행해졌다. 주입된 CO_2 의 모니터링을 위해서 그 지역에서 행해진 다양한 측정들 중, P 파 속도의 변화를 이용하여 2 개의 관측정 사이에서 대수층 내의 CO_2 분포를 알기 위해 시간차 시추공간 탄성파 토모그래피가 실시되었다. 이 논문은 탄성파 토모그래피에 대한 예비적인 결과들이다.

시추공간 탄성파 토모그래피 측정이 3 회에 걸쳐 실시되었는데, 한 번은 기준 조사로서 주입 전에, 나머지 두 번은 모니터링 조사를 위해 주입 중에 이루어졌다. 모니터링 조사로부터의 속도 분포도를 기준 조사 속도 분포도와 비교하여 속도 차 분포도가 만들어졌다. 속도 차 분포도는 주입된 CO_2 가 퍼져있다고 예상되는 주입정 주변 대수층 부분에서 속도 감소 지역을 보여준다.

비록 탄성파 토모그래피가 CO_2 주입에 따른 속도 감소 지역을 제공할 수 있었지만 속도 차 분포도에서 다소 이상한 속도 분포 지역이 관측되었다. 그러한 현상의 발생을 조사하기 위해서 조사 지역을 모사하는 수치모형 실험을 수행하였다. 그 결과 우리는 속도 차 분포도에서 발생한 이상한 속도 분포는 인위적인 오차이거나 이 지역에서 행해진 시추공간 탐사의 송수신기 배열에 의한 고스트라고 확신할 수 있었다. 토모그래피에 의해서 얻어진 최대 속도 감소 비율은 음파검층에 의해 관측된 것보다 아주 작았다. 비록 탄성파 토모그래피에 대한 수치모형 실험에 의해서도 불일치가 확인되었으나, 음파검층에 의해 획득한 속도 값에 비교될 수 있는 좀 더 정확한 속도 값을 얻기 위해 앞으로 더 많은 연구가 필요하다.

주요어： 시간차, 시추공간탐사, 탄성파 토모그래피, CO_2 주입, 육상 대수층

1 応用地質(株)
2 地球環境産業技術研究機構
3 エンジニアリング振興協会　石油開発環境センター

1 응용 지질㈜
2 Research Institute of Innovative Technology for the Earth
3 Safety and Environment Center for Petroleum Development, Engineering Advancement Association of Japan